Performance Comparison of Space Time Block Codes for Different 5G Air Interface Proposals

Sher Ali Cheema, Kristina Naskovska, Mohammadhossein Attar, Bilal Zafar, and Martin Haardt
Communication Research Laboratory
Ilmenau University of Technology, Germany
Email: {sher-ali.cheema, martin.haardt}@tu-ilmenau.de

(Invited paper for the special session on multiple antenna concepts for new 5G air interface proposals)

***Abstract*—Several new multi-carrier transmission techniques such as Filter Bank Multi-Carrier (FBMC), Universal Filtered Multi-Carrier (UFMC), and Generalized Frequency Division Multiplexing (GFDM) are being proposed as an alternative to orthogonal frequency division multiplexing (OFDM) for future wireless communication systems. Since multiple-input multiple-output (MIMO) will be an integral part of the 5th Generation (5G) cellular systems, the performance of these new schemes needs to be investigated for MIMO system. Space time block codes (STBC) are widely used in MIMO system because of their ability to achieve full diversity and the simple linear processing at the receiver. In this work, we propose two approaches for using STBCs in UFMC. Moreover, we also investigate the performance of these proposed schemes over frequency selective environments, and compare it with the performance of the other non-orthogonal techniques mentioned above.**

Keywords – 5th Generation (5G), Filter Bank Multi-Carrier (FBMC), Universal Filtered Multi-Carrier (UFMC), Generalized Frequency Division Multiplexing (GFDM), Orthogonal Frequency Division Multiplexing (OFDM)

I. Introduction

5th generation (5G) cellular communication systems are expected to support many application scenarios such as the tactile Internet, machine-type communications (MTC), Internet of things (IoT), and many more, on top of providing data rates of few Gigabits/s wireless connectivity. At present, orthogonal frequency division multiplexing (OFDM) is the standard waveform for the 4th generation (4G) cellular communication systems. OFDM requires a significant signaling overhead due to its strict synchronization requirements, which is a major shortcoming for the application scenarios being considered for the 5G systems. Therefore, different new waveforms with less stringent synchronization requirements are being proposed for the 5G air interface. The most well-known amongst these waveforms are Filter Bank Multi-Carrier (FBMC), Universal Filtered Multi-Carrier (UFMC), and Generalized Frequency Division Multiplexing (GFDM).

OFDM is a widely adopted solution mainly because of its robustness against multipath channels and its easy implementation. It is based on the Fast Fourier Transform (FFT) algorithm where the complete frequency band is digitally filtered as a whole. But OFDM is not spectrum efficient due to its utilization of guard band and a cyclic prefix (CP) to avoid inter-carrier interference (ICI) and inter-symbol interference (ISI), thus the time-frequency efficiency of OFDM is clearly below 1 [1]. Additionally, OFDM suffers from high out-of-band (OOB) emission which poses a challenge for opportunistic and dynamic spectrum access [2].

A solution to these problems was provided in the shape of FBMC where the filtering functionality is applied on a per subcarrier basis instead of applying it on the complete frequency band [3]. Any filter design with low OOB emission can be chosen. The subcarrier filters are very narrow in frequency and thus require long filter lengths. This causes the overlapping of symbols in time and hence a CP is not required. However, the requirement of a long filter length for FBMC makes it unsuited for communication in short uplink bursts, as required in many potential 5G application scenarios. OFDM and FBMC may be seen as the two extreme cases of a more general modulation paradigm where filtering is either applied on a complete band or on a per subcarrier basis. Therefore, in [1], a new multi-carrier waveform called Universal Filtered Multi-Carrier (UFMC) was proposed which is a generalization of OFDM and FBMC. Here, the filtering is applied on groups of subcarriers which allows for a significant reduction in the filter length as compared to FBMC.

Multiple-input multiple-output (MIMO) systems can multiply the overall radio link capacity and have hence become an integral part of present day communication systems. Space time block codes (STBC) are generally used in MIMO systems when no channel state information (CSI) is available at the transmitter. Therefore, in this work, we mainly focus on investigating the Alamouti STBC for the UFMC waveform. To the best of our knowledge, the performance of UFMC has not been investigated for MIMO systems. Moreover, in the literature, the performance of these newly proposed 5G air interfaces has not been compared with each other yet. Therefore, in this work, we compare the performance of UFMC not only with OFDM but also with GFDM (in the final version of the paper, the performance comparison with FBMC will also be included). Furthermore, we perform a comprehensive complexity analysis for the STBC schemes of

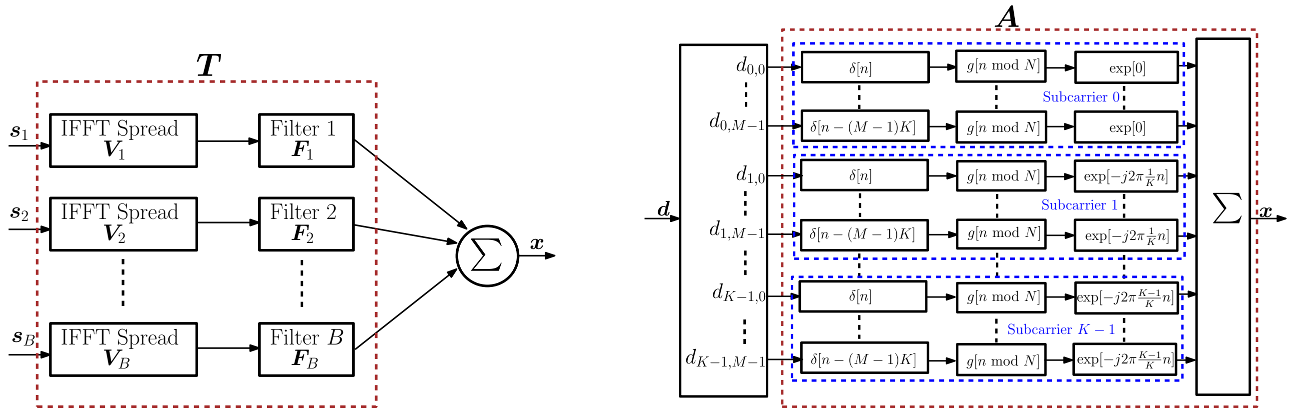

(a) UFMC modulator

(b) GFDM modulator

Fig. 1: Generation of UFMC and GFDM modulation waveform

these proposed 5G waveforms.

The organization of the remaining part of the paper is as follows. Section II describes the system model of UFMC and GFDM. In Section III, two proposed STBC schemes for UFMC are presented. Moreover, we also give an overview of STBC for GFDM. Section IV presents the complexity analysis for some of the proposed 5G air interface waveforms. Section V shows the simulation results and quantifies the system performance in terms of symbol error rate (SER) using LTE parameters. The paper is summarized at the end in Section VI.

Notation: The superscripts $(\cdot)^*$, $(\cdot)^{\mathrm{T}}$, $(\cdot)^{\mathrm{H}}$, and $(\cdot)^+$ represent complex conjugate, matrix transpose, complex conjugate transpose (Hermitian), and the Moore-Penrose pseudo-inverse, respectively. The operator diag(...) returns a block diagonal matrix with its arguments on the diagonal.

II. System Model

A. Universal Filtered Multi-Carrier

In UFMC, as shown in Fig. 1a, the overall K data subcarriers are grouped in B sub-bands where each sub-band comprises n_l subcarriers such that $K = Bn_l$. Each sub-band operation may be referred to as a UFMC sub-module. The i-th UFMC sub-module for $i = 1, ..., B$ takes $\boldsymbol{s}_i$ complex data symbols as input. The vector $\boldsymbol{s}_i$ includes n_l QAM symbols. Then an N_{FFT} point IFFT is applied on each sub-band to obtain the time domain signal. Afterwards, additional filtering is applied on each sub-band. For instance, a Dolph-Chebyshev filter maximizes the side lobe attenuation for a given main lobe width. Therefore, we have applied a Dolph-Chebyshev filter with N_{f} coefficients and side-lobe attenuation parameter α_{SLA}. The output for each UFMC module is then added together to form the transmit vector $\boldsymbol{x}$, given as,

$$\boldsymbol{x} = \sum_{i=1}^{B} \boldsymbol{x}_i = \sum_{i=1}^{B} \boldsymbol{F}_i \boldsymbol{V}_i \boldsymbol{s}_i, \tag{1}$$

where $\boldsymbol{V}_i \in \mathbb{C}^{N_{\text{FFT}} \times n_l}$ is the IFFT matrix which includes the relevant columns of the inverse Fourier matrix according to the respective sub-band position. The matrix $\boldsymbol{F}_i \in \mathbb{C}^{(N_{\text{FFT}}+N_{\text{f}}-1) \times N_{\text{FFT}}}$ is a Toeplitz matrix composed of the Dolph-Chebyshev filter impulse response which executes the linear convolution.

The transmit signal $\boldsymbol{x} \in \mathbb{C}^{(N_{\text{FFT}}+N_{\text{f}}-1)}$ can be rewritten using the following definitions:

$$\boldsymbol{F} = [\boldsymbol{F}_1, \boldsymbol{F}_2, \cdots, \boldsymbol{F}_B] \in \mathbb{C}^{(N_{\text{FFT}}+N_{\text{f}}-1) \times (B \times N_{\text{FFT}})}$$

$$\boldsymbol{V} = \text{diag}(\boldsymbol{V}_1, \boldsymbol{V}_2, \cdots, \boldsymbol{V}_B) \in \mathbb{C}^{(B \times N_{\text{FFT}}) \times K}$$

$$\boldsymbol{s} = [\boldsymbol{s}_1^T, \boldsymbol{s}_2^T, \cdots, \boldsymbol{s}_B^T]^T \in \mathbb{C}^K,$$

resulting in

$$\boldsymbol{x} = \boldsymbol{T}\boldsymbol{s} \in \mathbb{C}^{(N_{\text{FFT}}+N_{\text{f}}-1)}, \tag{2}$$

where $\boldsymbol{T} = \boldsymbol{F}\boldsymbol{V} \in \mathbb{C}^{(N_{\text{FFT}}+N_{\text{f}}-1) \times K}$ is the UFMC modulation matrix.

UFMC does not essentially require a CP but it can still be used to further improve the robustness against ISI. Assuming that the perfect time and frequency synchronization is accomplished and perfect channel state information is available at the receiver, the received signals $\boldsymbol{y}$ for the single-input single-output (SISO) system is

$$\boldsymbol{y} = \boldsymbol{H}\boldsymbol{x} + \boldsymbol{w} \in \mathbb{C}^{(N_{\text{FFT}}+N_{\text{f}}-1)}, \tag{3}$$

where $\boldsymbol{H}$ is channel convolution matrix and $\boldsymbol{w}$ is zero mean, complex additive white Gaussian noise. The channel estimation and equalization for UFMC is as simple as that for OFDM. Both processes can be performed in the frequency domain [1]. After the equalization the UFMC demodulation process is carried out which can be expressed as

$$\hat{\boldsymbol{s}} = \boldsymbol{U}\boldsymbol{y}_{\text{eq}}, \tag{4}$$

where $\hat{\boldsymbol{s}}$ represents the estimated data symbols, $\boldsymbol{U} \in \mathbb{C}^{K \times (N_{\text{fft}}+N_f-1)}$ is the UFMC demodulation matrix, and $\boldsymbol{y}_{\text{eq}}$ are the equalized symbols. Standard receiver options can be employed for the UFMC demodulator. It can be a matched filter (MF) receiver $\boldsymbol{U}_{\text{MF}} = \boldsymbol{T}^{\text{H}}$, or a zero forcing (ZF) receiver $\boldsymbol{U}_{\text{ZF}} = \boldsymbol{T}^+$ which completely removes the self interference.

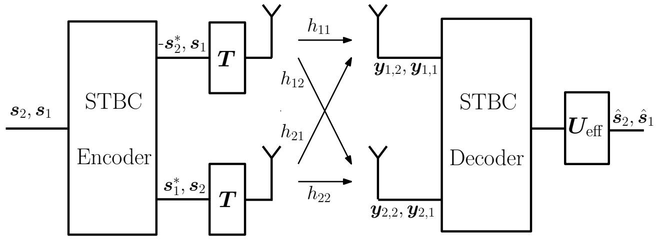

(a) Space-time coding on UFMC data carriers

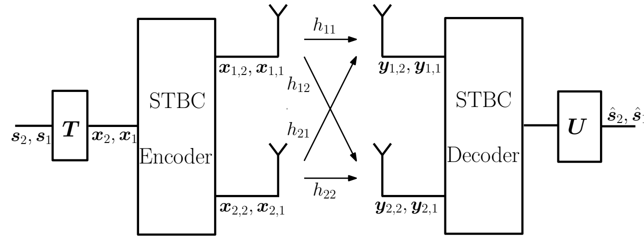

(b) TR-STC for UFMC

Fig. 2: Two approaches for Alamouti's STBC for UFMC waveform

B. Generalized Frequency Division Multiplexing

GFDM is a comparatively more flexible multicarrier scheme as it spreads the data symbols onto a time-frequency block and each subcarrier is filtered with a circular pulse shaping filter [4]. A block of N complex QAM data symbols is decomposed into K subcarriers with M subsymbols such that the total number of symbols follows $N = KM$. The vector $\boldsymbol{d}$ containing the N data symbols is grouped according to $d_{k,m} = [d_{0,0}, ..., d_{0,M-1}, ..., d_{K-1,M-1}]^{\text{T}}$ as shown in Fig. 1b. The subsymbols on each subcarrier are modeled as Dirac pulses that are K samples apart. Each $d_{k,m}$ is transmitted with the corresponding pulse shape

$$g_{k,m}[n] = g[(n - mK) \bmod N] \exp\left[-j2\pi \frac{k}{K} n\right]$$

where $g_{k,m}[n]$ is the transmit filter circularly shifted to the mth submsymbol and modulated to the kth subcarrier as shown in Fig. 1b. The overall GFDM transmit signal samples $x[n]$ of one block are given by

$$x[n] = \sum_{k=0}^{K-1} \sum_{m=0}^{M-1} g_{k,m}[n]\, d_{k,m} \qquad n = 0, 1, ..., N-1 \tag{5}$$

We can rewrite Eq. (5) into a matrix according to

$$\boldsymbol{x} = \boldsymbol{A}\boldsymbol{d}, \tag{6}$$

where $\boldsymbol{x}$ represents the transmit samples in time domain and $\boldsymbol{A}$ is the GFDM modulator matrix of size $KM \times KM$ with a structure according to

$$\boldsymbol{A}_{n+1,k+mK+1} = g_{k,m}[n].$$

A CP is added to the modulated signal to provide easy frequency domain equalization at the receiver. After passing through the wireless channel the received signal is given by Eq. (3). After removing the CP at the receiver, the frequency domain equalization can be performed. The equalized time domain samples $\boldsymbol{y}_{\text{eq}}$ are then passed through the GFDM demodulator, given as

$$\hat{\boldsymbol{d}} = \boldsymbol{B}\boldsymbol{y}_{\text{eq}}, \tag{7}$$

where $\boldsymbol{B} \in \mathbb{C}^{KM \times KM}$ is the GFDM demodulator matrix. Just like the UFMC demodulator, a MF receiver $\boldsymbol{B}_{\text{MF}} = \boldsymbol{A}^{\text{H}}$ or a ZF receiver $\boldsymbol{B}_{\text{ZF}} = \boldsymbol{A}^{+}$ can be used as a GFDM demodulator. Moreover, it has been shown in [5] that even in the absence of noise and channel, $\boldsymbol{B}_{\text{MF}}$ does not completely eliminate the crosstalk between different symbols and channels. Therefore, a corresponding interference cancellation scheme is required for the MF.

III. Space Time Block Codes

A. Space Time Block Coding for UFMC

In this section, we investigate the Alamouti STBC for the UFMC waveform using two transmit and receive antennas. Initially Alamouti STBC was designed for flat fading channels and the encoding rule was applied to two consecutive symbols instead of applying it to the blocks of data. Later on, in [6], Alamouti-based space-frequency coding for OFDM was proposed. Moreover, in [7], work on combining the Alamouti scheme with single carrier block transmission and frequency domain equalization was presented. Since additional filtering is applied to lower the OOB emission for the newly proposed 5G transmission schemes, therefore the transceiver architecture for the STBC differs to that of OFDM. In this work we propose two approaches, shown in Fig. 2, for the application of Alamouti STBCs for UFMC.

1) Approach 1: Here we investigate the space-time block coding for UFMC where coding is applied in the frequency domain on data carriers as is done for OFDM. Fig. 2a shows the simplified block diagram for the Alamouti STBC for a UFMC system using this approach. The modulated data symbols $\boldsymbol{s}$ are processed by the space-time encoder to produce the signals $\boldsymbol{s}_1$ and $\boldsymbol{s}_2$ for two transmit antennas in two successive time frames as shown in Table I.

	Antenna 1	Antenna 2
Time frame 1	$\boldsymbol{s}_1$	$\boldsymbol{s}_2$
Time frame 2	$-\boldsymbol{s}_2^*$	$\boldsymbol{s}_1^*$

TABLE I: STBC in frequency domain

The two data vectors at the output of the space-time encoder are independently modulated by the UFMC modulator matrix $\boldsymbol{T}$ according to Eq. (2) and then transmitted by the two antennas. On the receiver side, the received signal at the two receive antennas for two time frames can be written as

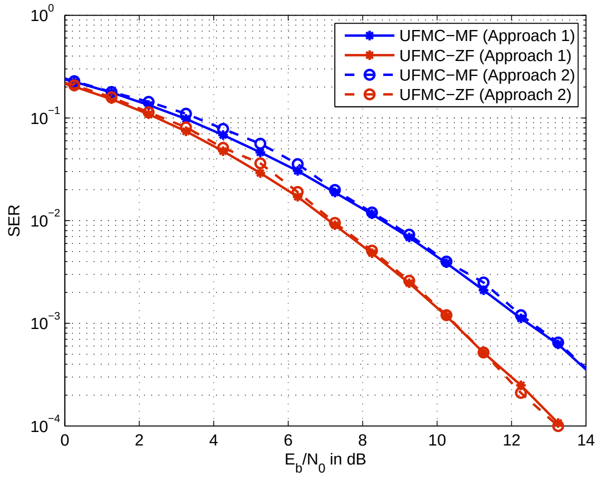

Fig. 3: SER performance of both STBC approaches for UFMC

$$\begin{bmatrix} \boldsymbol{y}_{1,1} \\ \boldsymbol{y}_{2,1} \end{bmatrix} = \begin{bmatrix} \boldsymbol{H}_{11}\boldsymbol{T} & \boldsymbol{H}_{12}\boldsymbol{T} \\ \boldsymbol{H}_{21}\boldsymbol{T} & \boldsymbol{H}_{22}\boldsymbol{T} \end{bmatrix} \begin{bmatrix} \boldsymbol{s}_1 \\ \boldsymbol{s}_2 \end{bmatrix} + \begin{bmatrix} \boldsymbol{w}_{1,1} \\ \boldsymbol{w}_{2,1} \end{bmatrix} \tag{8}$$

$$\begin{bmatrix} \boldsymbol{y}_{1,2} \\ \boldsymbol{y}_{2,2} \end{bmatrix} = \begin{bmatrix} \boldsymbol{H}_{11}\boldsymbol{T} & \boldsymbol{H}_{12}\boldsymbol{T} \\ \boldsymbol{H}_{21}\boldsymbol{T} & \boldsymbol{H}_{22}\boldsymbol{T} \end{bmatrix} \begin{bmatrix} -\boldsymbol{s}_2^* \\ \boldsymbol{s}_1^* \end{bmatrix} + \begin{bmatrix} \boldsymbol{w}_{1,2} \\ \boldsymbol{w}_{2,2} \end{bmatrix}, \tag{9}$$

where subscript $(.)_{i,j}$ in Eq. (8) and Eq. (9) represents receive antennas and time frames, respectively. Moreover, $\boldsymbol{H}_{ji} \in \mathbb{C}^{(N_{\text{FFT}}+N_{\text{ch}}+N_{\text{f}}-2)\times(N_{\text{FFT}}+N_{\text{f}}-1)}$ is the convolution matrix between the jth transmit antenna and the ith receive antenna. After taking the complex conjugate of Eq. (9) and rearranging with Eq. (8), we get the following result

$$\begin{bmatrix} \boldsymbol{y}_{1,1} \\ \boldsymbol{y}_{2,1} \\ \boldsymbol{y}_{1,2}^* \\ \boldsymbol{y}_{2,2}^* \end{bmatrix} = \boldsymbol{H}_{\text{eff}}\boldsymbol{T}_{\text{eff}} \begin{bmatrix} \boldsymbol{s}_1 \\ \boldsymbol{s}_2 \end{bmatrix} + \begin{bmatrix} \boldsymbol{w}_{1,1} \\ \boldsymbol{w}_{2,1} \\ \boldsymbol{w}_{1,2}^* \\ \boldsymbol{w}_{2,2}^* \end{bmatrix}, \tag{10}$$

where

$$\boldsymbol{H}_{\text{eff}} = \begin{bmatrix} \boldsymbol{H}_{11} & \boldsymbol{H}_{12} & \boldsymbol{0} & \boldsymbol{0} \\ \boldsymbol{H}_{21} & \boldsymbol{H}_{22} & \boldsymbol{0} & \boldsymbol{0} \\ \boldsymbol{0} & \boldsymbol{0} & \boldsymbol{H}_{12}^* & -\boldsymbol{H}_{11}^* \\ \boldsymbol{0} & \boldsymbol{0} & \boldsymbol{H}_{22}^* & -\boldsymbol{H}_{21}^* \end{bmatrix}$$

$$\boldsymbol{T}_{\text{eff}} = \begin{bmatrix} \boldsymbol{T} & \boldsymbol{0} \\ \boldsymbol{0} & \boldsymbol{T} \\ \boldsymbol{T}^* & \boldsymbol{0} \\ \boldsymbol{0} & \boldsymbol{T}^* \end{bmatrix}$$

are the $\boldsymbol{H}_{\text{eff}} \in \mathbb{C}^{4(N_{\text{FFT}}+N_{\text{ch}}+N_{\text{f}}-2)\times 4(N_{\text{FFT}}+N_{\text{f}}-1)}$ equivalent channel matrix and the $\boldsymbol{T}_{\text{eff}} \in \mathbb{C}^{4(N_{\text{fft}}+N_f-1)\times 2K}$ modulation matrix to be processed at the receiver for achieving diversity. The estimated data symbols $\hat{\boldsymbol{s}}$ may be achieved by applying space-time maximum ratio combining or ZF equalization using Eq. (10) in the frequency domain. The estimated symbols using ZF equalization can be written as

$$\hat{\boldsymbol{s}} = \boldsymbol{U}_{\text{eff}}(\boldsymbol{H}_{\text{eff}})^+ \begin{bmatrix} \boldsymbol{y}_{1,1} \\ \boldsymbol{y}_{2,1} \\ \boldsymbol{y}_{1,2}^* \\ \boldsymbol{y}_{2,2}^* \end{bmatrix}, \tag{11}$$

where $\boldsymbol{U}_{\text{eff}}$ is the effective UFMC demodulator matrix and it can be a MF demodulator $\boldsymbol{U}_{\text{eff}} = (\boldsymbol{T}_{\text{eff}})^{\text{H}}$ or ZF demodulator $\boldsymbol{U}_{\text{eff}} = (\boldsymbol{T}_{\text{eff}})^+$.

2) Approach 2: In [7], a time reversal space-time code (TR-STC) has been proposed for single carrier with frequency domain equalization (SC-FDE) transmission over frequency selective channels which is basically an extension of Alamouti's STBC. We propose to apply TR-STC on blocks of UFMC time domain samples as shown in Fig. 2b. The data symbols are first modulated using the UFMC modulator matrix $\boldsymbol{T}$ according to the Eq. (2) , then the time domain output signals $\boldsymbol{x}_1$ and $\boldsymbol{x}_2$ are processed by the space-time encoder according to Table III for $n = 0, 1, ..., N_l - 1$, where N_l is the length of UFMC modulated signal vectors $\boldsymbol{x}_1$ or $\boldsymbol{x}_2$. At the receiver side, the signal at the ith receiving antenna for the two time frames is

	Antenna 1	Antenna 2
Time frame 1	$x_{1,1}[n] = x_1[n]$	$x_{2,1}[n] = x_2[n]$
Time frame 2	$x_{1,2}[n] = -x_2^*[(-n)_{N_l}]$	$x_{2,2}[n] = x_1^*[(-n)_{N_l}]$

TABLE III: TR-STC for UFMC

$$\begin{aligned} \boldsymbol{y}_{i,1} &= \boldsymbol{H}_{1,i}\boldsymbol{x}_{1,1} + \boldsymbol{H}_{2,i}\boldsymbol{x}_{2,1} + \boldsymbol{w}_{i,1} \\ \boldsymbol{y}_{i,2} &= \boldsymbol{H}_{1,i}\boldsymbol{x}_{1,2} + \boldsymbol{H}_{2,i}\boldsymbol{x}_{2,2} + \boldsymbol{w}_{i,2}, \end{aligned} \tag{12}$$

where $\boldsymbol{H}_{j,i} \in \mathbb{C}^{(N_{\text{FFT}}+N_{\text{ch}}+N_{\text{f}}-2)\times(N_{\text{FFT}}+N_{\text{f}}-1)}$ is the convolution matrix between the jth transmit antenna and the ith receive antenna and $\boldsymbol{w}_{i,1}$ and $\boldsymbol{w}_{i,2}$ are the noise vectors for the two time frames. Both received signals are transformed into the frequency domain by applying FFT. Assuming that the channel remains constant for two time slots, we can rewrite Eq. (12) in the frequency domain as

$$\begin{bmatrix} \tilde{\boldsymbol{y}}_{1,1} \\ \tilde{\boldsymbol{y}}_{2,1} \\ \tilde{\boldsymbol{y}}_{1,2}^* \\ \tilde{\boldsymbol{y}}_{2,2}^* \end{bmatrix} = \tilde{\boldsymbol{H}}_{\text{eff}} \begin{bmatrix} \tilde{\boldsymbol{x}}_1 \\ \tilde{\boldsymbol{x}}_2 \end{bmatrix} + \begin{bmatrix} \tilde{\boldsymbol{w}}_{1,1} \\ \tilde{\boldsymbol{w}}_{2,1} \\ \tilde{\boldsymbol{w}}_{1,2}^* \\ \tilde{\boldsymbol{w}}_{2,2}^* \end{bmatrix}, \tag{13}$$

with

$$\tilde{\boldsymbol{H}}_{\text{eff}} = \begin{bmatrix} \tilde{\boldsymbol{H}}_{11} & \tilde{\boldsymbol{H}}_{12} \\ \tilde{\boldsymbol{H}}_{21} & \tilde{\boldsymbol{H}}_{22} \\ \tilde{\boldsymbol{H}}_{12}^* & -\tilde{\boldsymbol{H}}_{11}^* \\ \tilde{\boldsymbol{H}}_{22}^* & -\tilde{\boldsymbol{H}}_{21}^* \end{bmatrix},$$

where $\tilde{\boldsymbol{H}}_{ji} = \text{diag}(\bar{\boldsymbol{H}}_{ji})$, with $\bar{\boldsymbol{H}}_{ji}$ being the Fourier transform of the channel impulse response between the jth transmit antenna and the ith receive antenna. We can employ ZF or a minimum mean square error (MMSE) equalizer in the

Parameters	OFDM	UFMC	GFDM
Modulation Order	QPSK or 16 QAM		
LTE Bandwidth	5 MHz		
No. of transmit antennas	2		
No.of receive antennas	2		
Channel model	Ped-A or Veh-A		
Sampling frequency	7.68 MHz		
Subcarrier spacing	15 Khz	15 Khz	240 kHz
No. of subcarriers (K)	300	300	32
No. of subsymbols (M)			15
No. of subcarriers in a sub-band		12	
IFFT length N_{fft}	512	512	
CP duration	36 samples	36 samples (filter length -1)	32 samples
Pulse shaping	Rectangular	Dolph-Chebyshev α_{SLB} = 60	Root raised cosine α = 0.3

TABLE II: Simulation parameters.

frequency domain. Thus the estimated signal in the frequency domain using the ZF equalizer is

$$\tilde{\boldsymbol{x}} = (\tilde{\boldsymbol{H}}_{\text{eff}})^{+} \begin{bmatrix} \tilde{\boldsymbol{y}}_{1,1} \\ \tilde{\boldsymbol{y}}_{2,1} \\ \tilde{\boldsymbol{y}}^{*}_{1,2} \\ \tilde{\boldsymbol{y}}^{*}_{2,2} \end{bmatrix}. \tag{14}$$

The output of the space-time combiner is processed by the UFMC demodulator using Eq. (4) where $\boldsymbol{y}_{\text{eq}}$ is the inverse Fourier transform of $\tilde{\boldsymbol{x}}$.

B. Space Time Block Coding for GFDM

We can also apply space-time coding on data carriers or on time domain samples for GFDM. However, when STBCs are applied directly to the data symbols, the linear GFDM demodulator can not decouple the subcarriers and subsymbols because of the multipath propagation channel. Hence, it leads to a severe performance loss. Because of this reason, in [8], TR-STC has been recommended for GFDM when space-time coding is applied on blocks of GFDM samples. We have used the same approach in this work to evaluate the performance of GFDM.

IV. Complexity analysis

This section will be included in the final version of the paper.

V. Simulation Results

For the simulations, a 2×2 LTE MIMO system with a bandwidth of 5 MHz is considered. The 3GPP channel models Veh-A and Ped-A are used. The simulation parameters for the three waveforms are defined in Table II. It was assumed that all the resources are allocated to one user. The performance of these schemes is compared in terms of the symbol error rate (SER). Moreover, it is assumed that perfect synchronization and perfect channel state information is available at the receiver.

The SER performance of the two STBC approaches, described in Section III, over the 3GPP Veh-A channel model is shown in Fig. 3 for 16 QAM. The results show that both approaches have a similar performance but the computational complexity of Approach 1 is much higher than Approach 2. Moreover, a modified UFMC demodulator is needed if the STBC is applied on the data subcarriers (Approach 1).

The performance comparison of the STBCs for the UFMC, GFDM, and OFDM cases are shown in Fig. 4, for MF and ZF based receivers. Moreover, we present results for two different modulation orders, QPSK and 16 QAM, over the 3GPP Ped-A and Veh-A channel, as shown in Fig. 4a and Fig. 4b, respectively. The results show that when we use a lower modulation order, the UFMC MF performance is equivalent to the ZF receiver. The GFDM ZF receiver outperforms all of the schemes even for a highly frequency selective channel (Veh-A). This is due to the fact that the symbols in GFDM are efficiently spread over time and frequency and the CP is utilized in a better way (over a data block, instead of just one symbol), whereas the GFDM MF receiver shows the worst performance because it cannot resolve the ISI. For the case of GFDM, an increase in the value of the pulse shaping filter's roll-off factor (α) results in a worse performance. We have, however, shown the results for the case of a small α, because in a practical system setup α should be chosen small to neglect the noise enhancement factor [4]. The SER performance of UFMC is slightly better than OFDM since it normally does not use any CP. Furthermore, we can see that the performance of the UFMC MF receiver has slightly decreased when using the higher modulation order of 16 QAM.

VI. Conclusion

Different approaches for space-time coding for UFMC have been presented in this paper. We can either apply the STBC on the data carriers or the on time domain samples (TR-STC). The results show that both approaches yield similar reults but TR-STC is recommended for UFMC since it has a lower complexity. Moreover, GFDM outperforms UFMC and OFDM since it uses the CP more efficiently which leads to a better performance over frequency selective channels. However, MF based receivers exhibit a very bad performance in the case of GFDM.

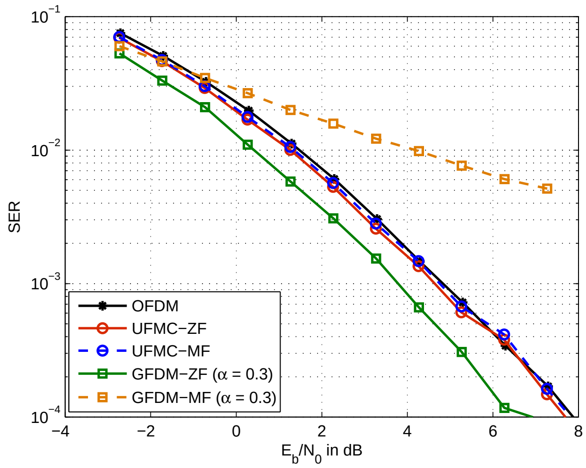

(a) SER performance for QPSK over Ped-A channel model

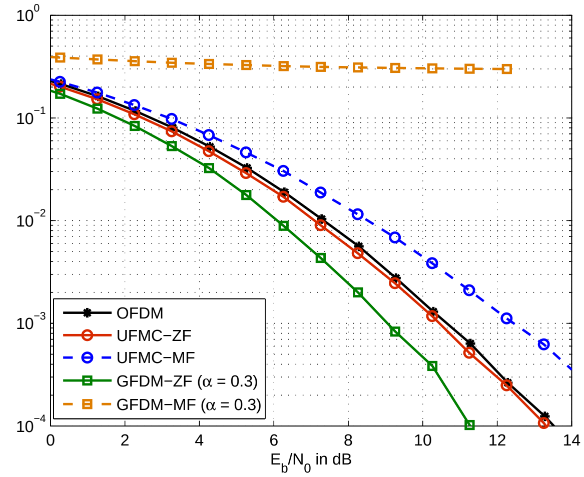

(b) SER performance for 16 QAM over Veh-A channel model

Fig. 4: SER performance for different 5G proposed transmission schemes

REFERENCES

[1] F. Schaich, T. Wild, and Y. Chen, "Waveform contenders for 5G - suitability for short packet and low latency transmissions," in *79th IEEE Vehicular Technology Conference (VTC Spring), 2014*, May 2014, pp. 1–5.

[2] E. Hossain, "Dynamic spectrum access and management in cognitive radio," *Cambridge University Press*, 2009.

[3] M. Bellanger, "Physical layer for future broadband radio systems," in *IEEE Radio and Wireless Symposium (RWS), 2010*, Jan 2010, pp. 436–439.

[4] N. Michailow, M. Matthe, I. Gaspar, A. Caldevilla, L. Mendes, A. Festag, and G. Fettweis, "Generalized frequency division multiplexing for 5th generation cellular networks," *IEEE Transactions on Communications,*, vol. 62, no. 9, pp. 3045–3061, Sept 2014.

[5] R. Datta, N. Michailow, M. Lentmaier, and G. Fettweis, "Gfdm interference cancellation for flexible cognitive radio phy design," in *IEEE Vehicular Technology Conference (VTC Fall), 2012*, Sept 2012, pp. 1–5.

[6] H. Bolcskei and A. Paulraj, "Space-frequency coded broadband OFDM systems," in *IEEE Wireless Communications and Networking Confernce, 2000. WCNC. 2000*, vol. 1, 2000, pp. 1–6 vol.1.

[7] N. Al-Dhahir, "Single-carrier frequency-domain equalization for space-time block-coded transmissions over frequency-selective fading channels," *IEEE Communications Letters,*, vol. 5, no. 7, pp. 304–306, July 2001.

[8] M. Matthe, L. Mendes, I. Gaspar, N. Michailow, D. Zhang, and G. Fettweis, "Multi-user time-reversal STC-GFDMA for future wireless networks," *EURASIP Journal on Wireless Communications and Networking*, vol. 2015, no. 1, 2015. [Online]. Available: http://dx.doi.org/10.1186/s13638-015-0366-6